J. Fluid Mech. (1984), *vol.* 142, *pp.* 9–37
Printed in Great Britain

On the propagation of waves exhibiting both positive and negative nonlinearity

By M. S. CRAMER AND A. KLUWICK†
Department of Engineering Science and Mechanics, Virginia Polytechnic Institute and State University, Blacksburg, Virginia 24061, U.S.A.

(Received 1 June 1983)

One-dimensional small-amplitude waves in which the local value of the fundamental derivative changes sign are examined. The undisturbed medium is taken to be a Navier–Stokes fluid which is at rest and uniform with a pressure and density such that the fundamental derivative is small. A weak shock theory is developed to treat inviscid motions, and the method of multiple scales is used to derive the nonlinear parabolic equation governing the evolution of weakly dissipative waves. The latter is used to compute the viscous shock structure. New phenomena of interest include shock waves having an entropy jump of the fourth order in the shock strength, shock waves having sonic conditions either upstream or downstream of the shock, and collisions between expansion and compression shocks. When the fundamental derivative of the undisturbed media is identically zero it is shown that the ultimate decay of a one-signed pulse is proportional to the negative $\frac{1}{3}$-power of the propagation time.

1. Introduction

A fundamental question in the study of nonlinear acoustics and gasdynamics concerns the nature of shock waves possible in any particular fluid. Over a wide range of pressures the only shock waves possible in many gases and liquids are in the form of compression shocks; i.e. discontinuities for which the pressure of a material particle increases in time. However, the existence of expansion shocks cannot be ruled out on purely thermodynamic grounds or from the point of view of stability. One therefore expects that materials will ultimately be encountered for which expansion shocks are not only possible but necessary. It is well known that compression shocks occur in fluids having a fundamental derivative $\bar{\Gamma} > 0$, and expansion shocks occur for those having $\bar{\Gamma} < 0$ (see e.g. Thompson 1971; Thompson & Lambrakis 1973). For our purposes it is convenient to write the fundamental derivative as

$$\bar{\Gamma}(\bar{\rho}, \bar{s}) \equiv \frac{1}{\bar{\rho}} \frac{\partial(\bar{a}\,\bar{\rho})}{\partial \bar{\rho}}\bigg|_{\bar{s}} = \frac{\bar{a}}{\bar{\rho}} + \frac{\partial \bar{a}}{\partial \bar{\rho}}\bigg|_{\bar{s}}, \tag{1.1}$$

where

$$\bar{a}(\bar{\rho}, \bar{s}) \equiv \left(\frac{\partial \bar{p}}{\partial \bar{\rho}}\bigg|_{\bar{s}}\right)^{\frac{1}{2}} \tag{1.2}$$

is the local sound speed and $\bar{\rho}$, $\bar{p}$, $\bar{s}$ are the local fluid density, pressure and entropy; throughout, dimensional quantities will be denoted by a bar. Thus most of the previous studies concerned with the existence of expansion shocks in single-phase fluids have simply analysed the variation of pressure with density.

† Permanent Address: Institut für Strömungslehre und Warmeübertragung, Technische Universität Wien, Wiedner Hauptstrasse 7, A-1040 Vienna, Austria.

Two of the earliest studies concerned with the existence of expansion shocks in gases are due to Bethe (1942) and Zel'dovich (1946), who showed that, for sufficiently high values of the specific heats, Van der Waals gases are capable of admitting expansion shocks. An important recent study is due to Thompson & Lambrakis (1973), who analysed the data of Martin & Hou (1955) and Hirschfelder *et al.* (1958) to give specific examples of real fluids having $\bar{\Gamma} < 0$. Finally, in the period of preparation of the present paper, Borisov *et al.* (1983) published direct experimental evidence of expansion shocks in Freon-13. Effects associated with negative nonlinearity are also known to occur in superfluid ^{4}He (see e.g. Osborne 1951; Temperley 1951; Khalatnikov 1952, 1956; Dessler & Fairbank 1956). Garrett (1981) has recently shown that finite-amplitude fourth sound waves in ^{3}He-B can also exhibit the positive and negative nonlinearity in the same disturbance. Although our main interest here is in single-phase fluids, we note that expansion shocks have also been observed in fused silica by Barker & Hollenback (1970). Bezzerides, Forslund & Lindman (1978) have also discussed such shocks in connection with two-fluid plasmas.

The above studies confirm that $\bar{\Gamma}$ can, in fact, change sign for a class of single-phase fluids. This occurs on a line in $(\bar{\rho}, \bar{s})$-space and, in this paper, we will refer to this as the transition line and its neighbourhood as the transition zone. When the undisturbed state is sufficiently far from this zone, every point on a given wave or pulse will correspond to either positive or negative values of $\bar{\Gamma}$. Here the wave behaviour is well known even when $\bar{\Gamma} < 0$, see e.g. Thompson 1971; Thompson & Lambrakis 1973). However, when the undisturbed state is sufficiently close to the transition line relative to the wave amplitude, the local value of $\bar{\Gamma}(\bar{\rho}, \bar{s})$ may change sign. As a result, one portion of the wave would correspond to $\bar{\Gamma} > 0$ and another to $\bar{\Gamma} < 0$, and the behaviour of the wave can be qualitatively different from that observed when the sign of Γ remains unchanged. This was first noticed by Thompson & Lambrakis (1973), who argued that these conditions could result in moderate-amplitude shock waves having sonic upstream and downstream conditions. Furthermore, Borisov *et al.* (1983) have correctly pointed out that a partial disintegration of a given initial shock may occur. However, this conclusion was based on a local and, it turns out, incorrect application of the classical Burgers equation; the correct analysis is given in the present study. In order to further our understanding of waves having both positive ($\bar{\Gamma} > 0$) and negative ($\bar{\Gamma} < 0$) nonlinearity, we have analysed the behaviour of one-dimensional small-amplitude waves propagating in a single-phase fluid whose undisturbed state lies in the transition zone. The disturbance size will be taken to be of the same order as that of the fundamental derivative. As a result, different portions of a wave may correspond to positive or negative values of $\bar{\Gamma}$. The fluid motions will be assumed to be governed by the usual Navier–Stokes equations; the thermodynamic variables and transport coefficients will be assumed to depend on two thermodynamic variables only, e.g. $\bar{\rho}$ and $\bar{s}$. Under certain circumstances, the regions of negative nonlinearity, i.e. those for which $\bar{\Gamma} < 0$, may include the critical point as well as regions of large thermal buoyancy. However, Thompson & Lambrakis (1973) have concluded that these effects may be negligible over a reasonable range of densities. Thus, in order to focus on the wave dynamics, we will follow these authors as well, as Borisov *et al.* (1983), in ignoring these effects.

In §2, the equations of motion are introduced and rewritten in terms of non-dimensional variables. In §3 we ignore dissipative effects and derive the equations governing waves which may include shock waves. This is recognized as a weak-shock theory analogous to that developed by Whitham (see e.g. Whitham 1974). Admissibi-

lity conditions for shock waves are discussed and it is found that the usual condition requiring an increase in entropy across the shock is not sufficient to rule out inadmissible discontinuities; the correct condition is given in terms of an ordering of the wave speeds along the lines suggested by Germain (1972). In §4 simple examples are used to illustrate the differences with the classical weak-shock theory. In §5 we include the effects of weak dissipation and derive the analogue of the Burgers equation. The shock structure is computed and it is shown that this no longer possesses the symmetry of the Taylor (1910) weak-shock structure.

2. Problem formulation

In this paper we consider fluids that are described by the classical Navier–Stokes equations. The unsteady one-dimensional version of these equations is

$$\bar{\rho}_{\bar{t}}+\bar{v}\,\bar{\rho}_{\bar{x}}+\bar{\rho}\bar{v}_{\bar{x}}=0, \tag{2.1}$$

$$\bar{\rho}(\bar{v}_{\bar{t}}+\bar{v}\bar{v}_{\bar{x}})+\bar{p}_{\bar{x}}=\{(\bar{\lambda}+2\bar{\mu})\,\bar{v}_{\bar{x}}\}_{\bar{x}}, \tag{2.2}$$

$$\bar{\rho}\bar{T}(\bar{s}_{\bar{t}}+\bar{v}\bar{s}_{\bar{x}})=(\bar{\lambda}+2\bar{\mu})\,\bar{v}_{\bar{x}}^2+(\bar{k}\bar{T}_{\bar{x}})_{\bar{x}}, \tag{2.3}$$

where $\bar{\rho}, \bar{p}, \bar{T}, \bar{S}$ and $\bar{v}$ denote the dimensional density, pressure, absolute temperature, entropy and velocity of the fluid. The quantities $\bar{k}$, $\bar{\mu}$ and $\bar{\lambda}$ are the dimensional thermal conductivity and first and second viscosities respectively. Equations (2.1)–(2.3) represent the usual conservation of mass, momentum and energy. In the inviscid limit, i.e. $\bar{\mu}, \bar{\lambda}, \bar{k}=0$, we must supplement the above differential equations with the following one-dimensional inviscid shock jump conditions:

$$\bar{u}[\bar{\rho}]=[\bar{\rho}\bar{v}], \tag{2.4}$$

$$(\bar{u}-\bar{v}_{\mathrm{a}})(\bar{u}-\bar{v}_{\mathrm{b}})=\frac{[\bar{p}]}{[\bar{\rho}]}, \tag{2.5}$$

$$[\bar{h}]=\tfrac{1}{2}(\bar{V}_{\mathrm{a}}+\bar{V}_{\mathrm{b}})[\bar{p}], \tag{2.6}$$

$$[\bar{s}]>0, \tag{2.7}$$

where $\bar{V}\equiv\bar{\rho}^{-1}$, and $\bar{h}$ and $\bar{u}$ are the specific enthalpy and shock speed. The brackets denote jumps, i.e. $[Q]\equiv Q_{\mathrm{a}}-Q_{\mathrm{b}}$, and the subscripts a and b refer to conditions after and before the shock. Equations (2.4) and (2.5) require that mass and momentum be conserved across the shock; (2.5) is recognized as the shock adiabat or Rankine–Hugoniot equation expressing conservation of energy, and (2.7) is the usual entropy inequality.

In all that follows we will take our dependent variables to be $\bar{\rho}(\bar{x},\bar{t})$, $\bar{s}(\bar{x},\bar{t})$ and $\bar{v}(\bar{x},\bar{t})$; the quantities $\bar{T}, \bar{p}, \bar{h}, \bar{k}, \bar{\mu}$ and $\bar{\lambda}$ will then be given as smooth functions of $\bar{\rho}, \bar{s}$ through state or constitutive relations. In the usual way, we will require that these constitutive relations satisfy the following inequalities for all values of $\bar{\rho}$ and $\bar{s}$ of interest:

$$\bar{\mu}\geqslant 0, \quad 2\bar{\mu}+3\bar{\lambda}\geqslant 0, \quad \bar{k}\geqslant 0 \tag{2.8}$$

and

$$\bar{c}_v\geqslant 0, \quad \left.\frac{\partial\bar{p}}{\partial\bar{\rho}}\right|_{\bar{T}}\geqslant 0, \tag{2.9}$$

where $\bar{c}_v$ is the specific heat at constant volume. The first set of inequalities are recognized as the conditions that the thermal conductivity, and the shear and bulk viscosities be positive. The second set of conditions corresponds to the conditions of

thermal and mechanical stability. When these are combined with the second law of thermodynamics, it is easily shown that

$$\bar{c}_p > \bar{c}_v \geqslant 0, \quad \left.\frac{\partial \bar{p}}{\partial \bar{\rho}}\right|_{\bar{s}} = \bar{\gamma}\left.\frac{\partial \bar{p}}{\partial \bar{\rho}}\right|_{\bar{T}} > 0, \tag{2.10}$$

where $\bar{c}_p$ is the specific heat at constant pressure, $\bar{\gamma} \equiv \bar{c}_p(\bar{\rho}, \bar{s})/\bar{c}_v(\bar{\rho}, \bar{s})$ and $\partial\bar{p}/\partial\bar{\rho}|_{\bar{s}}$ is recognized as the square of the sound speed given by (1.2).

As indicated in §1, the main objective of the present paper is to describe solutions to (2.1)–(2.3) in which the undisturbed state is within the transition region. Thus we will confine our attention to fluids in which $\bar{\Gamma} = \bar{\Gamma}(\bar{\rho}, \bar{s})$ changes sign and therefore which possess the transition region defined above.

The undisturbed state will be taken to be uniform and at rest, i.e. $\bar{v} = 0$, $\bar{\rho} = \rho_0$, $\bar{s} = s_0$, where the constants ρ_0 and s_0 are such that $\bar{\Gamma}(\rho_0, s_0) \approx 0$. It is therefore natural to non-dimensionalize the above equations such that

$$\begin{gathered}\bar{x} \equiv Lx, \quad \bar{t} \equiv La_0^{-1}t, \quad \bar{v} \equiv a_0 v, \quad \bar{\rho} \equiv \rho_0 \rho, \quad \bar{s} \equiv c_{v0}\, s, \\ \bar{p} \equiv \rho_0 a_0^2 p, \quad \bar{T} \equiv T_0 T, \quad \bar{\lambda} \equiv \lambda_0 \lambda, \quad \bar{\mu} \equiv \mu_0 \mu, \\ \bar{k} \equiv k_0 k, \quad \bar{u} \equiv a_0 u, \quad \bar{h} \equiv a_0^2 h, \quad \bar{V} \equiv \rho_0^{-1} V,\end{gathered}$$

where L gives a measure of the length of the disturbance, and the subscript 0 denotes quantities evaluated at the undisturbed state ρ_0, s_0, i.e. for any dimensional quantity $\bar{Q} = Q(\bar{\rho}, \bar{s})$, $Q_0 \equiv \bar{Q}(\bar{\rho}_0, \bar{s}_0)$. As a result, (2.1)–(2.3) become

$$\rho_t + v\rho_x + \rho v_x = 0, \tag{2.11}$$

$$\rho(v_t + vv_x) + p_x = \frac{1}{R}\left\{\left(\frac{\lambda_0}{\mu_0}\lambda + 2\mu\right)v_x\right\}_x, \tag{2.12}$$

$$\rho T(s_t + vs_x) = \frac{1}{R}\left\{E\left(\frac{\lambda_0}{\mu_0}\lambda + 2\mu\right)v_x^2 + \frac{\gamma_0}{Pr}(kT_x)_x\right\}, \tag{2.13}$$

where $\gamma_0 \equiv \bar{\gamma}(\rho_0, s_0)$ and

$$R \equiv \frac{\rho_0 a_0 L}{\mu_0}, \quad Pr \equiv \frac{\mu_0 c_{p0}}{k_0}, \quad E \equiv \frac{a_0^2}{T_0 c_{v0}};$$

these are, of course, just the Reynolds, Prandtl and Eckert numbers. The inviscid-shock jump conditions (2.4)–(2.7) now read

$$u[\rho] = [\rho v], \tag{2.14}$$

$$(u - v_a)(u - v_b) = \frac{[p]}{[\rho]}, \tag{2.15}$$

$$[h] = \tfrac{1}{2}(V_a + V_b)[p], \tag{2.16}$$

$$[s] \geqslant 0. \tag{2.17}$$

In the following sections we will take the dimensional perturbation density levels to be of order $\epsilon\rho_0$; as a result we will take

$$v = O(\rho - 1) = O(\epsilon) = o(1).$$

This will be assumed to be true at every point in the fluid; thus all shocks may be regarded as weak. In order that the undisturbed state lie in the vicinity of the transition line $\bar{\Gamma}(\rho_0, s_0) = 0$, we will also require

$$\Gamma \equiv \frac{\rho_0}{a_0}\bar{\Gamma}(\rho_0, s_0) = O(\epsilon) = o(1). \tag{2.18}$$

3. Weak-shock theory

In this section we discuss inviscid solutions, i.e. solutions in the limit $R \to \infty$, to the above equations of motion. When we ignore the right-hand sides of (2.12) and (2.13), the method of characteristics and standard thermodynamic identities may be used to show that

$$\rho \, \mathrm{d}v \pm a \, \mathrm{d}\rho = -\alpha s_x \, \mathrm{d}t \tag{3.1}$$

must be satisfied on

$$\frac{\mathrm{d}x}{\mathrm{d}t} = v \pm a, \tag{3.2}$$

where the non-dimensional function $\alpha = \alpha(\rho, s)$ is given by

$$\alpha \equiv \frac{c_{v0}}{\rho_0 a_0^2} \overline{\beta T \rho a^2}$$

and

$$\bar{\beta} \equiv -\frac{1}{\bar{\rho}} \frac{\partial \bar{\rho}}{\partial \bar{T}}\bigg|_{\bar{p}}.$$

The entropy s will be determined through the third characteristic relation

$$s = \text{constant} \quad \text{on} \quad \frac{\mathrm{d}x}{\mathrm{d}t} = v, \tag{3.3}$$

i.e. the entropy is constant on particle paths. Solutions to these characteristic relations generally result in shock formation. Once this occurs, (2.14)–(2.17) can be coupled with (3.1)–(3.3) to compute the resultant wave evolution.

In any theory involving the propagation of shocks of non-uniform strength, it is essential to take into account the entropy and entropy gradients generated by these shocks. For weak shocks in an arbitrary fluid, Bethe (1942) has expanded the Rankine–Hugoniot relation (2.6) to show that

$$[\bar{s}] = \frac{\bar{\Gamma}_{\mathrm{b}}}{6 \bar{T}_{\mathrm{b}} \bar{\rho}_{\mathrm{b}}^2 \bar{a}_{\mathrm{b}}^5} [\bar{p}]^3 + o([\bar{p}]^3), \tag{3.4}$$

provided that $\bar{\Gamma}_{\mathrm{b}} \neq 0$. However, in the case considered here, $\bar{\Gamma}$ is always of order $[\bar{p}]$. Thus higher-order terms in (3.4) can be of the same order as that shown. When we take (2.18) into account we find that the correct lowest-order expression for $[\bar{s}]$ can be written

$$[\bar{s}] = \frac{a_0^2 [\bar{\rho}]^3}{6 T_0 \rho_0^3} \left\{ \Gamma + \frac{\Lambda}{2} \left(\frac{\bar{\rho}_{\mathrm{b}} - \rho_0}{\rho_0} + \frac{\bar{\rho}_{\mathrm{a}} - \rho_0}{\rho_0} \right) \right\} + o\left\{ \left(\frac{\bar{\rho} - \rho_0}{\rho_0} \right)^4 \right\}, \tag{3.5}$$

where Γ is defined in (2.18) and

$$\Lambda \equiv \frac{\rho_0^2}{a_0} \frac{\partial \bar{\Gamma}}{\partial \bar{\rho}}\bigg|_{\bar{s}} (\rho_0, s_0). \tag{3.6}$$

Thus, in the transition zone, the size of the entropy jump across weak shocks is fourth order in the pressure jump. Not only does $[\bar{s}]$ depend on the value of $\bar{\Gamma}$ before the shock, but also on its rate of change along an isentrope. Furthermore, if $\bar{\Gamma} \equiv 0$ just before the shock, the sign of the entropy jump is always that of the derivative $\partial \bar{\Gamma} / \partial \bar{\rho}|_{\bar{s}}$ evaluated immediately before the shock. It will be shown later that (3.5) yields a simple relation between the entropy jump and the wave speeds on either side of the shock.

As in more conventional weak-shock theories, (3.3) may be used to argue that the primary source of entropy gradients is due to variations in the strength of any shock

waves embedded in the flow. We may therefore take our perturbation expansions to be of the general form

$$\left.\begin{aligned} v &= \epsilon v_1 + \epsilon^2 v_2 + \epsilon^3 v_3 + o(\epsilon^3), \\ \rho &= 1 + \epsilon\rho_1 + \epsilon^2\rho_2 + \epsilon^3\rho_3 + o(\epsilon^3), \\ s &= s_0/c_{v0} + \epsilon^4 s_4 + o(\epsilon^4). \end{aligned}\right\} \tag{3.7}$$

We now note that the lowest-order analysis of (3.1), (3.2), (2.14) and (2.15) shows that the variation of the shock strength is only noticeable over times and propagation distances of order ϵ^{-2} rather than ϵ^{-1}. Thus, for propagation times of order ϵ^{-2}, the integral

$$\int_0^t s_x(x,\tau)\,\mathrm{d}\tau$$

evaluated on a characteristic defined by (3.2) is of the order of $[s]$, i.e. ϵ^4 at most. Thus, for the present purposes, the entropy-gradient term appearing in (3.1) is seen to be negligible. When this fact is taken into account and the expansions (3.7) are substituted in (3.1), (3.2), (2.14) and (2.15), we find that the perturbation equations corresponding to (3.1) and (3.2) are

$$\mathrm{d}(v_1 \pm \rho_1) = 0 \tag{3.8}$$

and

$$\mathrm{d}(v_2 \pm \rho_2) + \rho_1\,\mathrm{d}(v_1 \mp \rho_1) = 0 \tag{3.9}$$

on

$$\frac{\mathrm{d}x}{\mathrm{d}t} = \pm 1 + \epsilon(v_1 \mp \rho_1) + \epsilon^2\{v_2 \mp \rho_2 \pm \hat{\Gamma}\rho_1 \pm (1 + \tfrac{1}{2}\Lambda)\rho_1^2\} + o(\epsilon^2), \tag{3.10}$$

and those corresponding to (2.14) are seen to be

$$[v_1 - \rho_1] = 0, \tag{3.11}$$

$$[v_2 - \rho_2 + \rho_1 v_1] = u_1[\rho_1], \tag{3.12}$$

where $\hat{\Gamma} \equiv \epsilon^{-1}\Gamma = O(1)$ and

$$u_1 \equiv -\tfrac{1}{2}(v_{1\mathrm{a}} - \rho_{1\mathrm{a}} + v_{1\mathrm{b}} - \rho_{1\mathrm{b}}). \tag{3.13}$$

In the derivation of (3.11) and (3.12), we have expanded (2.15) to obtain an approximation for the shock speed u appearing in (2.14). Here we restrict our attention to right-moving shocks, i.e. shocks that propagate in the positive x-direction. For this case, the expansion for u is found to be

$$u \sim 1 + \epsilon u_1 + \epsilon^2 u_2 + o(\epsilon^2),$$

where u_1 is given by (3.13) and u_2 is defined by

$$u_2 = \frac{1}{2}\left\{v_{2\mathrm{a}} + v_{2\mathrm{b}} + \frac{[\rho_2][\rho_1^2]}{[\rho_1]^2} - 2\frac{[\rho_1\rho_2]}{[\rho_1]} + \frac{[v_1]^2}{4} - \frac{[\rho_1^2]^2}{4[\rho_1]^2} + \hat{\Gamma}\frac{[\rho_1^2]}{[\rho_1]} + (1 + \tfrac{1}{3}\Lambda)\frac{[\rho_1^3]}{[\rho_1]}\right\}.$$

From (3.8) it is clear that $v_1 - \rho_1$ is a constant on the left-running characteristics defined by (3.10). Furthermore, (3.11) implies that this Riemann invariant is also continuous across right-running shock waves. In the present study, we are only interested in cases for which the fluid is undisturbed sufficiently far ahead of any shock waves. As a result, $v_1 = \rho_1$ everywhere, including behind shocks. Thus (3.13) requires that $u_1 = 0$, and (3.8) and (3.10) require that $\rho_1 =$ constant on

$$\frac{\mathrm{d}x}{\mathrm{d}t} = 1 + \epsilon^2(v_2 - \rho_2 + \hat{\Gamma}\rho_1 + (1 + \tfrac{1}{2}\Lambda)\rho_1^2) + o(\epsilon^2).$$

Thus, in order to compute the distortion in the right-moving characteristics, we need to calculate the variation in v_2 and ρ_2 as well. The arguments that led to the above relation between v_1 and ρ_1 may now be applied to (3.9) and (3.12) to show that $v_2 = \rho_2 - \rho_1^2$ everywhere. Thus the characteristic relations reduce to

$$\rho_1 = \text{constant}, \tag{3.14}$$

on

$$\frac{\mathrm{d}x}{\mathrm{d}t} = 1 + \epsilon^2(\hat{\Gamma} + \tfrac{1}{2}\Lambda\rho_1)\,\rho_1 + o(\epsilon^2). \tag{3.15}$$

The analogous result for 4th sound in ^{3}He-B has been derived by Garrett (1981). Because of (3.14) it is clear that the right-moving characteristics (3.15) are always straight lines in the (x,t)-plane. Furthermore, the shock speed can now be written

$$u = 1 + \tfrac{1}{2}\epsilon^2\left\{\hat{\Gamma}\frac{[\rho_1^2]}{[\rho_1]} + \tfrac{1}{3}\Lambda\frac{[\rho_1^3]}{[\rho_1]}\right\} + o(\epsilon^2),$$

or, equivalently,

$$u = 1 + \tfrac{1}{2}\epsilon^2\{\hat{\Gamma}(\rho_{1\mathrm{a}} + \rho_{1\mathrm{b}}) + \tfrac{1}{3}\Lambda(\rho_{1\mathrm{a}}^2 + \rho_{1\mathrm{a}}\rho_{1\mathrm{b}} + \rho_{1\mathrm{b}}^2)\} + o(\epsilon^2). \tag{3.16}$$

As in the classical weak-shock theory, (3.14)–(3.16) may be used to compute the details of a wide variety of initial- and boundary-value problems. This can be done by computing the flow field exactly with (3.14) and (3.15). The motion of any discontinuities can then be calculated through use of (3.16). Alternatively, we can also make use of an area rule analogous to that of Whitham (see e.g. Whitham 1974). We have found that such an area rule may be derived under fairly general conditions; this has been worked out in the Appendix.

We now note two special cases; in the first $|\Lambda\rho_1|$ is negligible compared with $|\hat{\Gamma}|$, and in the second $\hat{\Gamma} = 0$ and $\Lambda \neq 0$. In the first case the variation of $\bar{\Gamma}(\bar{\rho}, \bar{s})$ with density along an isentrope is negligible, at least to the order considered. As a result, the local value of $\bar{\Gamma}$ is effectively independent of the size of the perturbation ρ_1, and the wave behaviour is the same as the case where $\bar{\Gamma}$ is an order-one constant. As pointed out by the previous investigators, the only discontinuities possible are expansion shocks when $\bar{\Gamma} < 0$ and compression shocks when $\bar{\Gamma} > 0$.

In the second case, the undisturbed state is on the transition line. For $\Lambda > 0$ portions of a wave having $\rho_1 < 0$ have local values of $\bar{\Gamma}$ that are less than zero, and those having $\rho_1 > 0$ correspond to values of $\bar{\Gamma}$ greater than zero. This case is recognized as being mathematically analogous to that considered by Lee-Bapty (1981) and Crighton (1982), and we therefore refer the reader there for further examples.

It is also of interest to note that when $\hat{\Gamma} \equiv 0$ and $\hat{\rho}_{\mathrm{b}} \equiv 0$ (3.16) may be combined with (3.15) to show that

$$u - 1 = \frac{1}{3}\left(\left.\frac{\mathrm{d}x}{\mathrm{d}t}\right|_{\mathrm{a}} - 1\right).$$

Thus, in a coordinate system moving with the undisturbed sound speed, the shock speed is a third rather than a half of the wave speed immediately after the shock.

As indicated by the above special cases and the examples of §4, solutions to (3.14)–(3.16) can be quite complicated and may involve phenomena not possible in the conventional weak-shock theory. At this stage it is useful to discuss the types of discontinuities possible near the transition line $\bar{\Gamma}(\bar{\rho}, \bar{s}) = 0$.

Certainly, a necessary condition for the existence of any discontinuity is that it can be formed through the steepening of an initially smooth pulse. As an example,

we note that such a mechanical condition eliminates the possibility of expansion shocks in fluids having $\bar{\Gamma} > 0$ everywhere and compression shocks in fluids having $\bar{\Gamma} < 0$. A simple way to check this is to compute the shock-formation time associated with (3.14) and (3.15). It is easily shown that a portion of an initially smooth density distribution $\rho_1 = \rho_1(x, 0)$ first results in infinite slopes, i.e. infinite values of $\rho_{1x}(x, t)$, when

$$t = -\frac{1}{\epsilon^2 \rho_{1x}(x,0)\,(\hat{\Gamma} + \Lambda \rho_1(x,0))}, \tag{3.17}$$

where the maximum of the absolute value of the denominator is to be taken; the latter condition determines where on the profile the shock first forms. Positive shock formation times correspond to negative values of the product

$$\rho_{1x}(x,0)\,(\hat{\Gamma} + \Lambda \rho_1(x,0));$$

thus both expansion shocks ($\rho_{1x}(x,0) > 0$) and compression shocks ($\rho_{1x}(x,0) < 0$) are possible, depending on the value of $\rho_1(x,0)$ relative to the constants $\hat{\Gamma}$ and Λ. In §4, the shock-formation process is illustrated through use of simple examples.

A second requirement for the existence of a discontinuity is that a physically realizable structure can be constructed; this condition is discussed further in §5, where the continuum shock structure is delineated. Finally, if a discontinuity is already embedded in a flow, a reasonable requirement is that the speed of the shock (3.16) lies between the wave speeds on either side; i.e. that

$$\left.\frac{\mathrm{d}x}{\mathrm{d}t}\right|_{\mathrm{a}} > u > \left.\frac{\mathrm{d}x}{\mathrm{d}t}\right|_{\mathrm{b}}, \tag{3.18}$$

where $\mathrm{d}x/\mathrm{d}t|_{\mathrm{a}}$ and $\mathrm{d}x/\mathrm{d}t|_{\mathrm{b}}$ are the quantities (3.15) evaluated at $\rho_{1\mathrm{a}}$ and $\rho_{1\mathrm{b}}$ respectively. Condition (3.18) has been suggested by Germain (1972), and is equivalent to the entropy condition of Lax (1971). This ensures that the conditions at the shock depend in an appropriate way on the initial conditions. The results (3.15) and (3.16) may be used to show that (3.18) is completely compatible with both compression and expansion shocks.

Although the condition (3.18) has been written in terms of inequalities, we have found that shocks having speeds equal to one wave-speed or the other are not only possible, but in some cases necessary. This is analogous to the Chapman–Jouguet point in the theory of detonation and deflagration shocks (see e.g. Hayes 1960; Courant & Friedrichs 1948), and has also been predicted by Lee-Bapty (1981) and Crighton (1982) in the context of viscoelastic waves. In the following we will refer to these conditions simply as sonic conditions. If (3.15) is combined with (3.16), the following useful result may be derived

$$\left.\frac{\mathrm{d}x}{\mathrm{d}t}\right|_{\mathrm{a}} - u = \frac{[\rho_1]}{4}\Lambda\epsilon^2\left(\rho_{1\mathrm{a}} + \frac{\hat{\Gamma}}{\Lambda}\right) + \frac{1}{2}\left(u - \left.\frac{\mathrm{d}x}{\mathrm{d}t}\right|_{\mathrm{b}}\right).$$

Furthermore, if sonic conditions hold after the shock, these same equations may be used to show that

$$[\rho_1] = 3\left(\rho_{1\mathrm{a}} + \frac{\hat{\Gamma}}{\Lambda}\right).$$

Thus, when $\Lambda > 0$, these results may be used to show that sonic conditions can occur after the shock only if

$$u < \left.\frac{\mathrm{d}x}{\mathrm{d}t}\right|_{\mathrm{b}}.$$

Because this contradicts the second inequality in (3.18), we reject this possibility and conclude that, when $A > 0$, sonic conditions can only occur before the shock; it is easily verified that this latter possibility is completely consistent with (3.18). Thus, when $A > 0$, we will take as our generalization of (3.18) the requirement that

$$\left.\frac{dx}{dt}\right|_a > u \geqslant \left.\frac{dx}{dt}\right|_b. \tag{3.19}$$

We may show by similar reasoning that, when $A < 0$, sonic conditions are only possible after the shock. As a result, when $A < 0$, we will take the generalization of (3.18) to be

$$\left.\frac{dx}{dt}\right|_a \geqslant u > \left.\frac{dx}{dt}\right|_b. \tag{3.20}$$

We have also found that it is possible to rewrite the conditions (3.19) and (3.20) directly in terms of the density perturbations before and after the shock. In order to present our results as concisely as possible, we will define

$$\hat{\rho} = \frac{A}{\bar{\Gamma}}\rho_1, \tag{3.21}$$

which will be useful as long as both $\hat{\Gamma}$ and A are non-zero. Conditions (3.19) and (3.20) may now be used to show that the permissible values of $\hat{\rho}_a$ and $\hat{\rho}_b$ lie between the lines $\hat{\rho}_b = \hat{\rho}_a$ and $\hat{\rho}_b = -\frac{1}{2}(\hat{\rho}_a + 3)$ for $A > 0$, and between $\hat{\rho}_b = \hat{\rho}_a = -2(\hat{\rho}_a + 3)$ for $A < 0$. The precise regions are depicted in figure 1; the shaded regions denote forbidden $(\hat{\rho}_a, \hat{\rho}_b)$-pairs, and values of $\hat{\rho}_a$ and $\hat{\rho}_b$ in the unshaded regions represent shock waves satisfying either (3.19) or (3.20). A similar diagram can be constructed for the case $\hat{\Gamma} \equiv 0$ with $A \neq 0$, and when $A \equiv 0$ with $\hat{\Gamma} \neq 0$ the forbidden region is given simply by the half-space $\hat{\Gamma}[\rho_1] < 0$.

It is also of interest to note that, when (3.15) is combined with (3.5), we obtain the following relation between the non-dimensional entropy jump and the jump in the wave speed:

$$[s] \sim \frac{a_0^2}{6T_0 c_{v0}} \epsilon^2 [\rho_1]^2 \left[\frac{dx}{dt}\right] + o(\epsilon^4),$$

where

$$\left[\frac{dx}{dt}\right] \equiv \left.\frac{dx}{dt}\right|_a - \left.\frac{dx}{dt}\right|_b = \epsilon^2 [\rho_1] \{\hat{\Gamma} + \tfrac{1}{2} A(\rho_{1a} + \rho_{1b})\}.$$

Because $\bar{T}$ is the absolute temperature and because of the inequalities (2.10) we see that the entropy increases across all discontinuities satisfying (3.19) or (3.20). However, unless $A \equiv 0$, the entropy inequality (2.17) does not necessarily imply (3.19) or (3.20). Thus, unless $A \equiv 0$, with $\hat{\Gamma} \neq 0$, the conditions (3.19) and (3.20) are seen to be stronger than (2.17); remarks similar to these are found in Hayes (1960).

In their analysis of kinematic waves, Lighthill & Whitham (1955) have pointed out that results such as (3.14)–(3.16) could be represented graphically by plotting the quantity

$$\hat{\jmath} \equiv \tfrac{1}{2}\hat{\rho}^2(1 + \tfrac{1}{3}\hat{\rho}) \tag{3.22}$$

versus $\hat{\rho}$; a plot of this is found in figure 2. It is easily verified that

$$\frac{d\hat{\jmath}}{d\hat{\rho}} = \frac{A}{\epsilon^2 \hat{\Gamma}}\left(\frac{dx}{dt} - 1\right)$$

and that

$$\frac{[\hat{\jmath}]}{[\hat{\rho}]} = \frac{A}{\epsilon^2 \hat{\Gamma}^2}(u - 1);$$

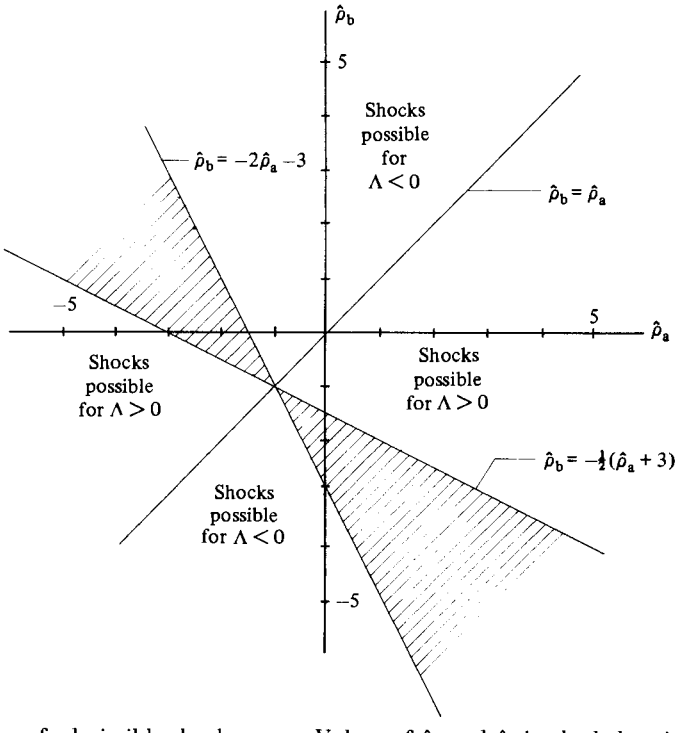

FIGURE 1. Regions of admissible shock waves. Values of $\hat{\rho}_a$ and $\hat{\rho}_b$ in shaded regions violate (3.19) and (3.20). The line $\hat{\rho}_b = -\frac{1}{2}(\hat{\rho}_a + 3)$ corresponds to sonic conditions before the shock.

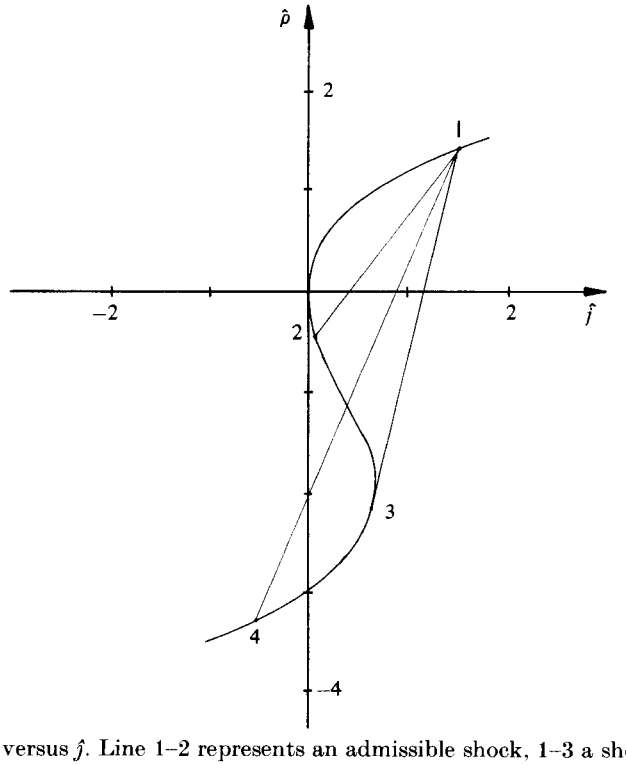

FIGURE 2. Plot of $\hat{p}$ versus $\hat{f}$. Line 1–2 represents an admissible shock, 1–3 a shock having sonic conditions at 3, and 1–4 an inadmissible shock.

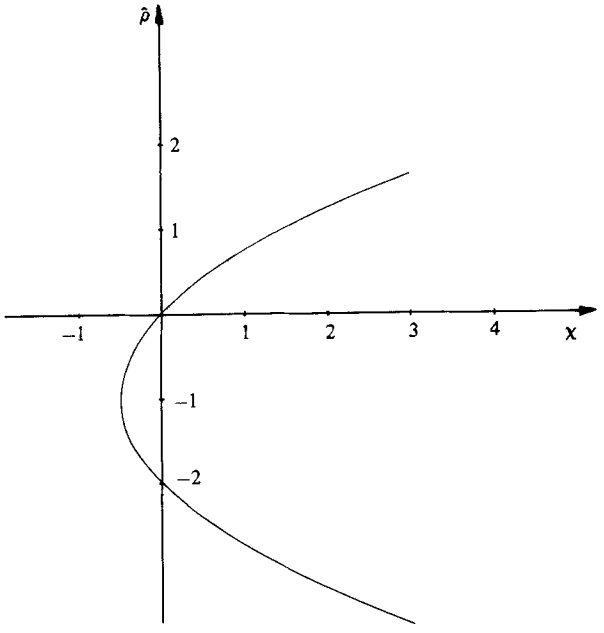

FIGURE 3. Structure of centred fans; $\chi \equiv (\hat{x}-\hat{x}_0)\,\hat{t}^{-1}$.

that is, the slope of this curve is directly related to the slope of the characteristic lines, and the slope of a straight line connecting any two points on this curve is essentially the shock speed corresponding to a shock having jump $[\rho_1]$. Shock waves having sonic conditions correspond to shock lines that are tangent to the $(\hat{\jmath},\hat{\rho})$-curve. Furthermore, an analysis of (3.19) and (3.20) or, equivalently, figure 1, shows that only shocks that do not cut the $(\hat{\jmath},\hat{\rho})$-curve can satisfy (3.19) or (3.20); such an inadmissible construction is given by the line 1–4 in figure 2.

The analogue of (3.22) valid when $A \equiv 0$ with $\hat{\Gamma} \neq 0$ is $j = \frac{1}{2}\rho_1^2\hat{\Gamma}$, which corresponds to the $\hat{\rho} \approx 0$ region of figure 2. When $\hat{\Gamma} \equiv 0$ with $A \neq 0$ the analogue is $j = \frac{1}{3}\rho_1^3 A$. This purely odd function could be approximated by the large-$|\hat{\rho}|$ behaviour of (3.22).

Inspection of (3.15) or figure 2 clearly indicates that the slopes of the characteristic lines have a local maximum or minimum at $\rho_1 = -\hat{\Gamma}/A$. This plays an important role in the analysis of specific examples. In particular, centred expansion or compression fans have limitations on their strength and may need to be supplemented with expansion or compression shocks having sonic conditions before or after the shock. Thus to conclude this section we will give a brief discussion of the structure of centred fans (figure 3). Because of (3.14), the characteristics are always straight lines, and, in the fan, will all be taken to be emanating from the point $x = x_0$, $t = 0$. We may then integrate (3.15) and invert to express the density perturbation ρ_1 as a function of space and time. The resultant expression for ρ_1 can be written

$$\rho_1 = -\frac{\hat{\Gamma}}{A} \pm \left\{\frac{\hat{\Gamma}^2}{A^2} + \frac{2}{\epsilon^2 A}\frac{x-t-x_0}{t}\right\}^{\frac{1}{2}},$$

or, if we define

$$\hat{t} \equiv \epsilon^2 t, \quad \hat{x} \equiv \frac{A}{\hat{\Gamma}^2}(x-t), \tag{3.23}$$

this may be rewritten as

$$\hat{\rho} = -1 \pm \left(1 + 2\frac{\hat{x} - \hat{x}_0}{\hat{t}}\right)^{\frac{1}{2}}, \tag{3.24}$$

where $\hat{x}_0 \equiv x_0 \Lambda / \hat{\Gamma}^2$ and $\hat{\rho}$ is given by (3.21). The distribution (3.24) is a parabola having an axis of symmetry $\rho_1 = -\hat{\Gamma}/\Lambda$ or $\hat{\rho} = -1$. This contrasts with the linear distribution found in conventional weak-shock theories. A second difference is that two distinct types of fan are possible. The first allows smooth transitions between any two points in the range $-1 < \hat{\rho}$ and the second between two points in the range $\hat{\rho} < -1$. Larger transitions, e.g. between $\hat{\rho} = 0$ and $\hat{\rho} = -\frac{3}{2}$, cannot be achieved by a single centred fan; in the examples of §4 we shall see that a shock–fan combination may be sufficient to carry out the desired transition.

4. Weak-shock theory: examples

Because of the large number of cases to be considered, it will be convenient to present our results in terms of the variables defined by (3.21) and (3.23). The equations of the characteristics (3.15), shock speed (3.16) and conditions on the relative wave speeds (3.19) and (3.20) may now be rewritten as

$$\frac{\mathrm{d}\hat{x}}{\mathrm{d}\hat{t}} = \hat{\rho} + \tfrac{1}{2}\hat{\rho}^2, \tag{4.1}$$

$$\frac{\mathrm{d}\hat{x}_\mathrm{s}}{\mathrm{d}\hat{t}} = \tfrac{1}{2}(\hat{\rho}_\mathrm{a} + \hat{\rho}_\mathrm{b}) + \tfrac{1}{6}(\hat{\rho}_\mathrm{a}^2 + \hat{\rho}_\mathrm{a}\hat{\rho}_\mathrm{b} + \hat{\rho}_\mathrm{b}^2), \tag{4.2}$$

and

$$\left.\frac{\mathrm{d}\hat{x}}{\mathrm{d}\hat{t}}\right|_\mathrm{a} > \frac{\mathrm{d}\hat{x}_\mathrm{s}}{\mathrm{d}\hat{t}} \geqslant \left.\frac{\mathrm{d}\hat{x}}{\mathrm{d}\hat{t}}\right|_\mathrm{b}, \tag{4.3}$$

where $\hat{x}_\mathrm{s} = \hat{x}_\mathrm{s}(\hat{t})$ is the position of a shock. These variables clearly give a natural representation of the wave dynamics, and we will refer to these as universal variables.

The obvious advantage of universal variables is that we may present one set of results instead of four sets corresponding to each permutation of the signs of $\hat{\Gamma}$ and Λ. For example, if, in universal variables, $\hat{\rho} = f(\hat{x}, \hat{t})$, then

$$\rho_1 = \frac{\hat{\Gamma}}{\Lambda} f\left(\frac{\Lambda}{\hat{\Gamma}^2}(x-t), \epsilon^2 t\right).$$

If we consider plots of ρ_1 versus $x-t$ with t fixed, it is clear that the plots for $\Lambda > 0$, $\hat{\Gamma} > 0$ will simply be stretched versions of the $\hat{\rho}$ versus $\hat{x}$ plots. The plots for $\hat{\Gamma} < 0$, $\Lambda > 0$ may then be obtained by reflection about the $(x-t)$-axis and those for $\hat{\Gamma} > 0$, $\Lambda < 0$ may be obtained by reflection about the ρ_1 axis. The results for $\hat{\Gamma} < 0$ and $\Lambda < 0$ clearly will require reflection about both axes. It is important to note that the conditions before the shock become those after the shock and *vice versa* when the sign of Λ is changed; when this is noted it is easily seen that the single condition (4.3) is completely equivalent to the two conditions (3.19) and (3.20). However, the exchanging of the after and before conditions comes out naturally and causes no difficulty if we are simply transforming results already obtained in universal variables to those involving ρ_1, x and t.

In the remainder of this section we will use the term expansion to refer to an increase in $\hat{\rho}$ with respect to $\hat{x}$, and compression to refer to a decrease in $\hat{\rho}$. Although the actual density variation may be exactly the opposite, this again comes out naturally in the transformation process and should cause no confusion.

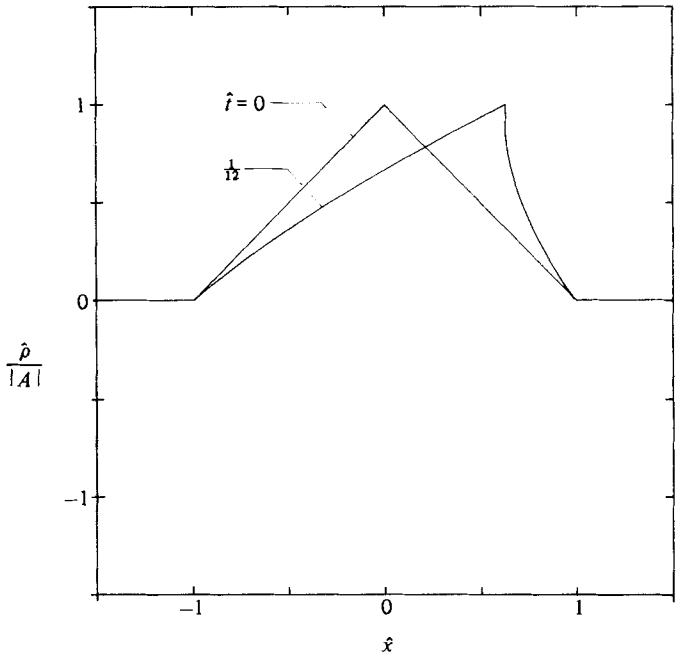

FIGURE 4. Shock formation for $A = 3.0$. Compression shock forms at peak.

Our first set of examples is designed to describe the process of shock formation. In order to emphasize the differences between the present theory and classical weak-shock theory we have examined the behaviour of a triangle wave having initial density distribution

$$\hat{\rho}(\hat{x},0) = \begin{cases} A(1-\hat{x}) & (0 \leqslant \hat{x} \leqslant 1), \\ A(1+\hat{x}) & (-1 \leqslant \hat{x} \leqslant 0), \\ 0 \quad \text{otherwise.} \end{cases}$$

In each case the profiles and shock formation times were computed with (4.1) and (3.17), and the profile(s) at formation were plotted along with the initial condition. In figure 4 the case $A = 3$ has been plotted; this is typical of all cases having $A > 0$. When $A > 0$, $\hat{\Gamma} > 0$ the local value of $\overline{\Gamma}$ is greater than zero everywhere; as a result the profile steepens forward, forming a compression shock. However, because the slope of the characteristic lines depends nonlinearly on $\hat{\rho}$, the initially straight lines in figure 4 become parabolas and the shock forms at the point of maximum amplitude, i.e. at the characteristic originating at $\hat{x} = 0$, with zero initial strength. Because the initial strength is zero, the shock speed (4.2) can be approximated by

$$\frac{\mathrm{d}\hat{x}_\mathrm{s}}{\mathrm{d}\hat{t}} \approx \tfrac{1}{2}(\hat{\rho}_\mathrm{a}+\hat{\rho}_\mathrm{b}),$$

and immediately after formation the propagation can be computed with the usual angle bisection rule (Whitham 1974).

In figure 5 the behaviour of the case where $A = -0.75$ is depicted. In this case the distortion is to the left, indicating that the local wave speed is everywhere less than the undisturbed sound speed. Here the compression shock forms not at the point of maximum $|\hat{\rho}|$, but on the characteristic originating at $\hat{x} = -1$.

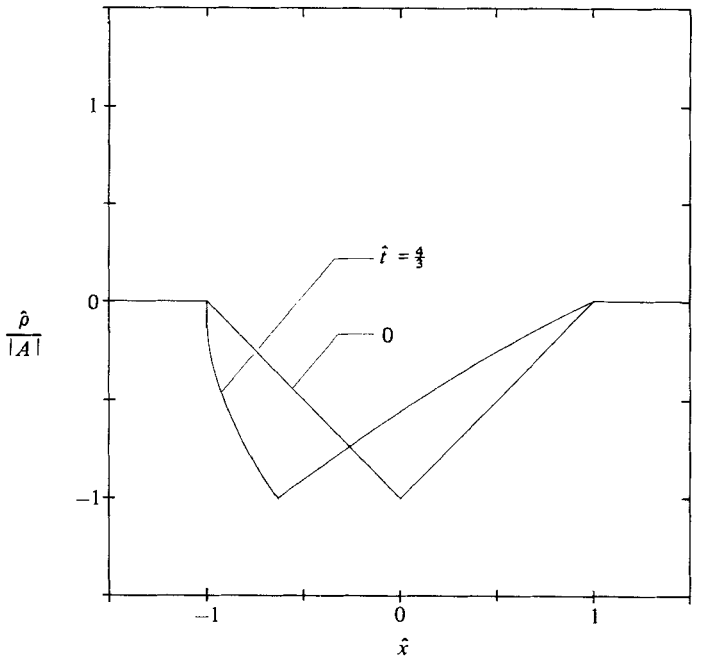

FIGURE 5. Shock formation for $A = -0.75$. Compression shock forms at $\hat{x} = -1$.

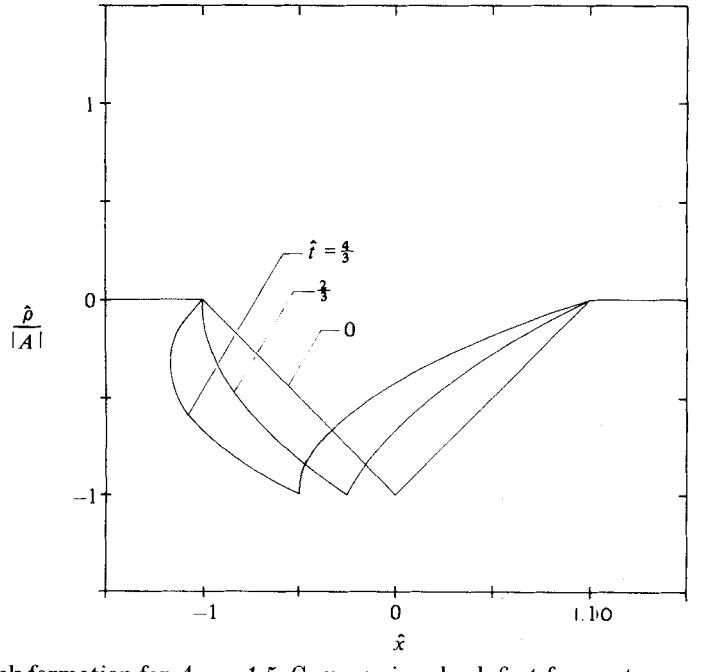

FIGURE 6. Shock formation for $A = -1.5$. Compression shock first forms at $x = -1$ and expansion shock then forms on characteristic originating at $x = 0$.

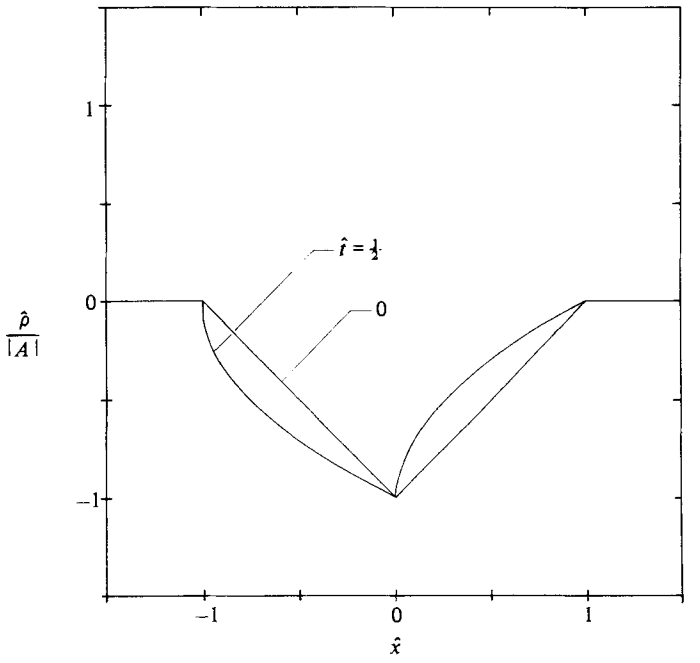

FIGURE 7. Shock formation for $A = -2.0$. Both compression and expansion shocks form at same time.

When $A < -1$ the sign of $\bar{\Gamma}$ is different in different parts of the wave. We therefore cannot expect even qualitative agreement with classical weak-shock theory. In figure 6 the evolution of a wave having $A = -1.5$ has been plotted. Here we find that a compression shock first forms at $\hat{t} = \frac{2}{3}$ on the characteristic originating at $\hat{x} = -1$. A second expansion shock then forms at $\hat{t} = \frac{4}{3}$ and at the point of maximum $|\hat{\rho}|$.

In figures 7 and 8 the behaviour of waves having even smaller values of A have been depicted. Although the number and types of shocks generated are the same as in figure 6, the nonlinear dependence of the wave speed (4.1) on $\hat{\rho}$ results in new features which are also of interest in flows having discontinuities even at $\hat{t} = 0$.

In figure 7 the case $A = -2$ has been plotted. The shock formation time for both shocks is the same, and, because the wave speed (4.1) corresponding to $\hat{\rho} = -2$ is also zero relative to the sound speed of the undisturbed medium, the expansion shock forms at $\hat{x} = 0$. When $A < -2$ portions of the wave having $-2 < \hat{\rho} < 0$ propagate at a speed smaller than that on the undisturbed medium and portions having $\hat{\rho} < -2$ propagate at a larger speed, resulting in the profiles plotted in figure 8. For $A < -2$ the expansion shock always forms first and the compression shock at $\hat{x} = -1$ second.

In the case $A = 0$ and $\hat{\Gamma} \neq 0$ the shock formation process is essentially the same as in the classical weak-shock theories where the triangle wave remains a triangle and the initial strength of the shock is equal to A. In the case $A \neq 0$, $\hat{\Gamma} \equiv 0$ and initial condition

$$\rho_1(x, 0; A) = \begin{cases} A\left(1 - \dfrac{x}{A}\right) & \left(0 < \dfrac{x}{A} < 1\right), \\ A\left(1 + \dfrac{x}{A}\right) & \left(-1 < \dfrac{x}{A} < 0\right), \\ 0 \quad \text{otherwise}, \end{cases}$$

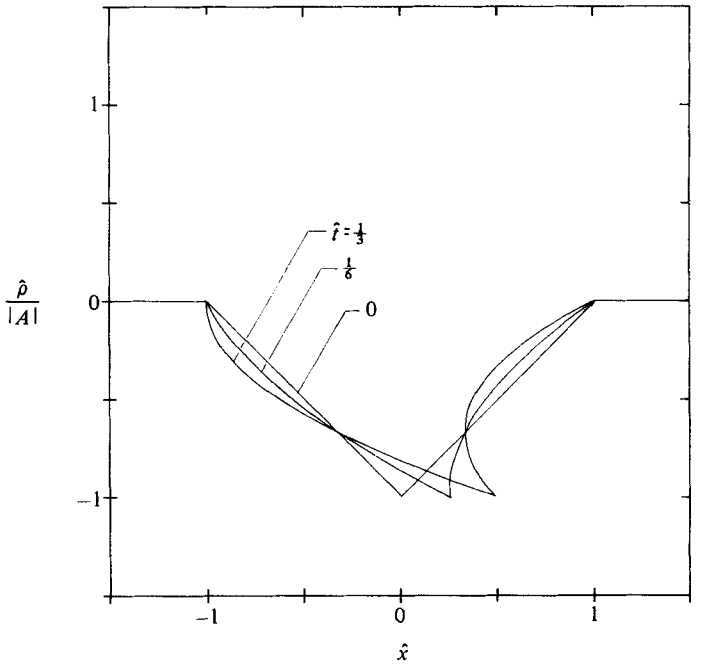

FIGURE 8. Shock formation for $A = -3.0$. Expansion shock first forms and compression shock then forms at $x = -1$.

the wave behaviour for $A > 0$ is essentially the same as that seen in figure 4. For $A > 0$ the wave steepens forward to form a compression shock at the peak of the wave, and for $A < 0$ the steepening is to the left to form an expansion wave; in both cases the shock forms when $t = (\epsilon A)^{-2}$. The propagation for $A < 0$ is identical with that for $A > 0$; in each case the latter profile simply needs to be reflected about the $(x-t)$-axis in a plot of ρ_1 versus $x-t$.

To illustrate the behaviour of shock waves we now discuss square pulses corresponding to the initial condition

$$\hat{\rho} = \begin{cases} A & (-1 \leqslant \hat{x} \leqslant 1), \\ 0 & \text{otherwise.} \end{cases}$$

The subsequent evolution will be computed using (4.1) and (4.2), and the inequalities (4.3) used to eliminate inadmissible discontinuities. When $A > 0$ the wave behaves as indicated in figure 9. Initially the compression shock propagates to the right with a constant speed of

$$\tfrac{1}{2}A(1+\tfrac{1}{3}A).$$

The expansion fan emanating from $\hat{x} = -1$ eventually catches the shock, resulting in a monotonic decay of the strength and speed of the shock. If we define $\hat{\rho}_a = F(\hat{t})$ to be a measure of the shock strength, the decay law is found to be given by the following implicit equation:

$$\hat{t}F^2(F+\tfrac{3}{2}) = 6A. \tag{4.4}$$

Once $F(\hat{t})$ is obtained from (4.4), the position of the shock is given by

$$\hat{x}_s = -1 + \frac{6A(2+F)}{F(3+2F)}.$$

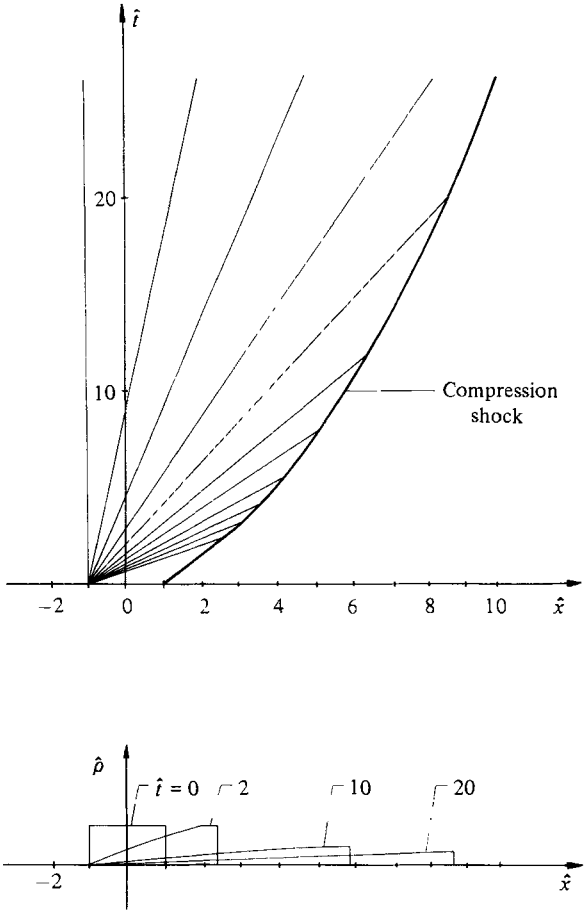

FIGURE 9. Wave evolution for $A = 1.0$.

Provided that $\hat{\Gamma} \neq 0$, (4.4) may be used to show that, as $\hat{t} \to \infty$,

$$\hat{\rho}_a \sim 2\left(\frac{A}{\hat{t}}\right)^{\frac{1}{2}} + o(\hat{t}^{-\frac{1}{2}}),$$

which is essentially the same decay law as in the classical theory.

When $-1 < A < 0$, the behaviour of the wave is again essentially the same as in the classical theory; this is illustrated in figure 10 for the case $A = -0.9$. When $A < -1$ the transition from $\hat{\rho} = 0$ to $\hat{\rho} = A$ cannot be achieved through a single expansion fan centred at $\hat{x} = 1$ (see e.g. figure 3). For $-\frac{3}{2} < A < -1$ the overall wave structure is essentially that of figure 11; here we see that an expansion shock must be inserted between the constant-density region and the fan emanating from $\hat{x} = 1$. The value of $\hat{\rho}$ after the shock is A, and before the shock the conditions must be sonic. As a result, the density before this shock is

$$\hat{\rho}_b = -\tfrac{1}{2}(A+3) > -1, \tag{4.5}$$

and the shock strength and speed are given by

$$[\hat{\rho}] = \tfrac{3}{2}(A+1), \quad \frac{d\hat{x}_s}{d\hat{t}} = -\tfrac{1}{8}(A+3)(1-A).$$

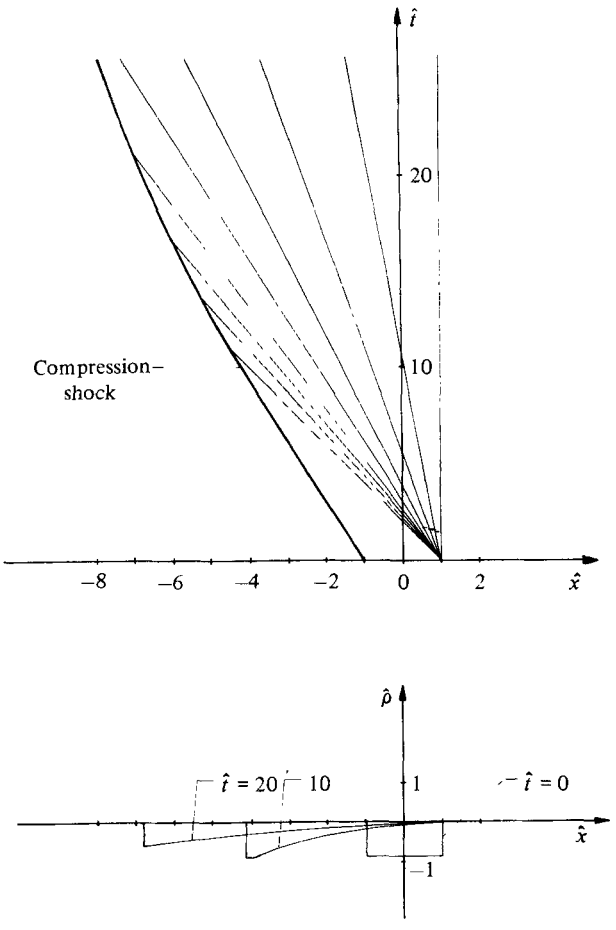

FIGURE 10. Wave evolution for $A = -0.9$.

For this range of A the expansion shock propagates with a constant strength and speed until it collides with the compression shock originating at $\hat{x} = -1$; the time at which this occurs is $48(A+3)^{-2}$. Immediately after the collision we find that only a single shock exists; i.e. the collision results in a merging of the expansion and compression shocks. The density perturbation immediately after the shock is therefore zero, the perturbation before the shock is just (4.5) and the resultant shock speed is

$$\frac{\mathrm{d}\hat{x}_s}{\mathrm{d}\hat{t}} = \tfrac{1}{24}(A^2-9). \tag{4.6}$$

It is easily shown that the absolute value of (4.6) is always less than that of the original compression shock. Thus the new shock formed by the merging process is slower, at least in the $(\hat{x}, \hat{t})$-plane, than either of the original shocks. As a result, the interaction with the expansion fan will continually slow this shock and cause it to decay. The equation governing the interaction is similar to (4.4) and the ultimate decay will again be governed by the classical $\hat{t}^{-\frac{1}{2}}$ law.

We note that when $A = -\frac{3}{2}$ the speed of the compression shock originating at $\hat{x} = -1$ is exactly equal to the wave speed just before the shock. If $|A|$ is increased

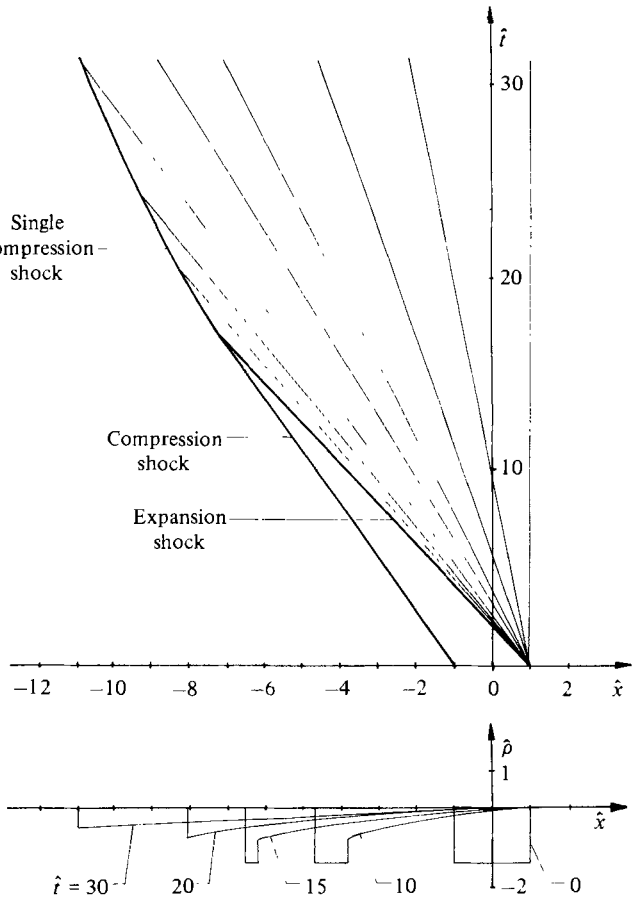

FIGURE 11. Wave evolution for $A = -1.4$.

beyond $\frac{3}{2}$ the inequality (4.3) can no longer be satisfied for a single shock having $\hat{\rho}_a = 0$ and $\hat{\rho}_b = A$. The correct wave behaviour for cases having $-3 < A < -\frac{3}{2}$ has been plotted in figure 12. The compression from $\hat{\rho} = A$ to $\hat{\rho} = 0$ is accomplished first through a compression fan and then through a compression shock. Before this shock sonic conditions hold, and just after we have $\hat{\rho}_a = 0$. Thus, the strength and speed of this shock are

$$[\hat{\rho}] = -\hat{\rho}_b = \tfrac{3}{2}, \quad \frac{d\hat{x}_s}{d\hat{t}} = -\tfrac{3}{8}; \tag{4.7}$$

these are the same for all values of $A < -\frac{3}{2}$. The structure of the compression fan seen in figure 12 is given by choosing the lower sign and $\hat{x}_0 = -1$ in (3.24); this is essentially the lower branch of the parabola found in figure 3. The expansion shock originating at $\hat{x} = 1$ will penetrate this fan at time

$$\hat{t} = \hat{t}_0 = \frac{16}{3}\frac{1}{(A+1)^2}.$$

The resultant interaction will decrease the strength of the expansion shock such that

$$[\hat{\rho}] = \tfrac{3}{2}(1+A)\left(\frac{\hat{t}_0}{\hat{t}}\right)^{\frac{3}{8}}. \tag{4.8}$$

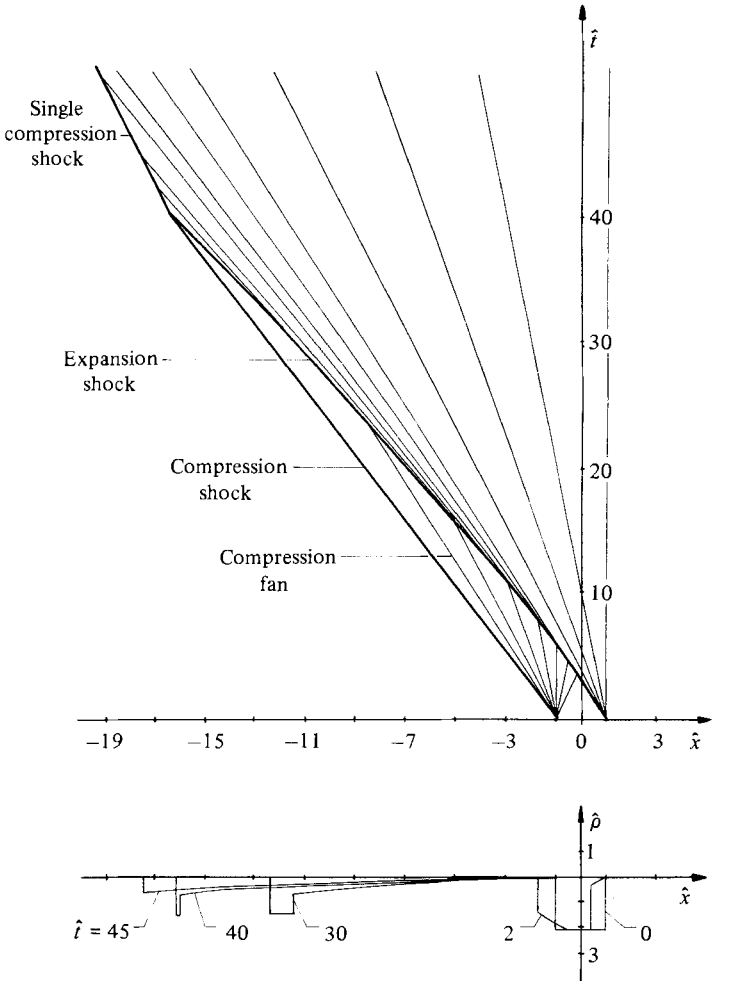

FIGURE 12. Wave evolution for $A = -2.2$.

After the interaction begins, the expansion fan originating at $\hat{x} = 1$ will no longer be followed by an expansion shock but a smooth precursor wave which in turn is followed by the expansion shock. The expansion and compression shock ultimately collide at time

$$(\hat{t} = \hat{t}_0(-2(1+A))^{\frac{8}{3}},$$

and merge to form a single compression shock. An instant before the collision, the compression shock is described by (4.7) and expansion shock is given by

$$\hat{\rho}_a = -\tfrac{3}{2}, \quad \hat{\rho}_b = -\tfrac{3}{4}, \quad \frac{d\hat{x}_s}{d\hat{t}} = -\tfrac{15}{32}$$

for all A in the interval of interest. Immediately after the collision we take $\hat{\rho}_a = 0$ and $\hat{\rho}_b = -\frac{3}{4}$, which from (4.2) yields a shock speed

$$\frac{d\hat{x}_s}{d\hat{t}} = -\tfrac{9}{32},$$

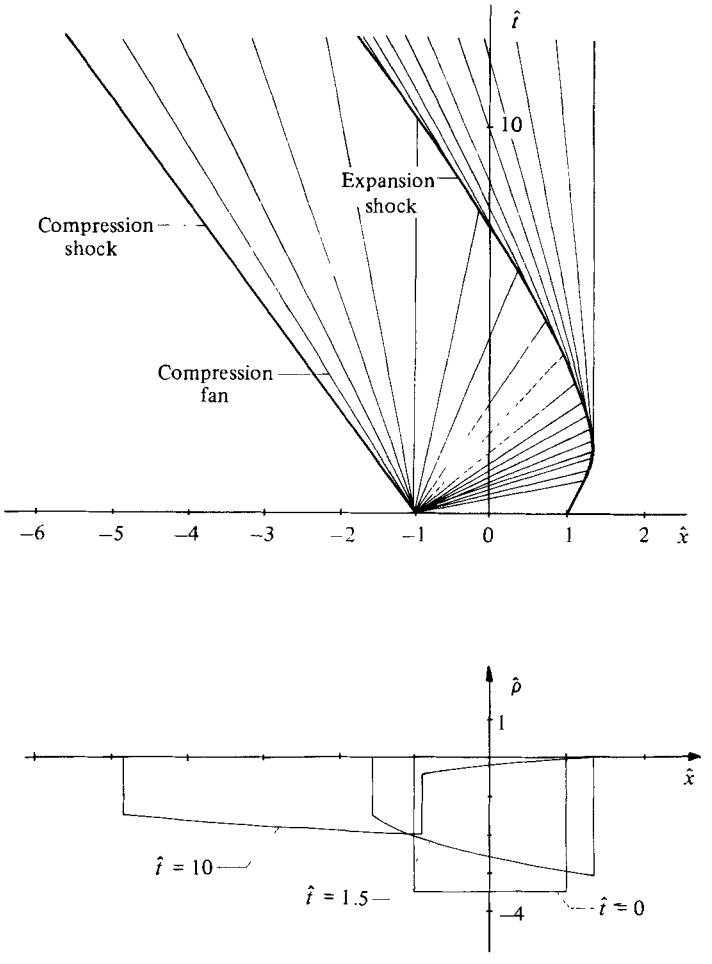

FIGURE 13. Wave evolution for $A = -3.5$.

which again implies that the speed of the new shock is larger, i.e. less negative, than that of the merging shocks immediately before the collision. Owing to interaction with the precursor and, later, with the centred fan, the shock then decays to acoustic conditions at infinity.

In figure 13 the wave structure typical of cases having $A < -3$ has been plotted. The new feature here is that the expansion shock originating at $\hat{x} = 1$ must now propagate in the positive $\hat{x}$-direction. The expansion fan at $\hat{x} = 1$ is no longer present and the initial shock speed is computed by substituting $\hat{\rho}_a = A$, $\hat{\rho}_b = 0$ in (4.2). The interaction with the compression fan slows the shock, which becomes stationary in the $(\hat{x}, \hat{t})$-plane when $\hat{\rho}_a = -3$. After this time, the shock moves to the left and its strength is given by an expression similar to (4.8). The subsequent details are essentially the same as those seen in figure 12, and, in particular, the details of the collision and merging of the expansion and compression shock are identical with the case $-3 < A < -\frac{3}{2}$.

The special cases where either A or $\hat{\Gamma}$ are zero have also been examined. As expected, the case $\hat{\Gamma} \neq 0$, $A = 0$ is essentially the same as the classical theory, and the case $\hat{\Gamma} = 0$, $A \neq 0$ closely resembles the cases described above in the limit $|A| \to \infty$.

However, in the latter case the shock–fan interaction results in a different decay law than the $t^{-\frac{1}{2}}$ law of the classical theory. For a square pulse we find that

$$[\rho_1] = Kt^{-\frac{1}{3}},$$

for all values of t after the interaction begins; here K is the usual integration constant. Thus, when $\Gamma \equiv 0$, the asymptotic decay rate is much smaller than that of the classical theory. In general, when $\hat{\Gamma} = 0$, $\Lambda \neq 0$, a one-signed smooth pulse always generates a single shock for which

$$[\rho_1] \sim \left(\frac{3M}{\Lambda \hat{t}}\right)^{\frac{1}{3}} + o(\hat{t}^{-\frac{1}{3}}) \tag{4.9}$$

as $\hat{t} \to \infty$, where $\hat{t}$ is given by (3.23) and

$$M \equiv \int_{-\infty}^{\infty} \rho_1(\zeta, 0)\, \mathrm{d}\zeta.$$

When $\Lambda > 0$ we may take $\rho_{1b} \approx 0$ in (4.9), and, when $\Lambda < 0$, ρ_{1a} can be neglected.

5. Dissipative effects

To derive the equation governing the evolution of weakly dissipative waves, (2.11)–(2.13) will be approximated through use of the method of multiple scales. As in the previous sections, we will confine our attention to small-amplitude solutions and therefore make use of the expansions (3.7). However, because the dissipative terms on the right-hand sides of (2.12) and (2.13) generate an order-ϵ^3 perturbation to the entropy, the expansion for s is (3.7) will be replaced by

$$s = \frac{s_0}{c_{v0}} + \epsilon^3 s_3 + o(\epsilon^3).$$

In order that the effects of dissipation be noticeable over the same timescales as the nonlinearity, we will require that $R = O(\epsilon^{-2})$ rather than ϵ^{-1}. In order that the undisturbed state be in the vicinity of the transition region, we will also require that (2.18) be satisfied. This, of course, is not used explicitly until the pressure and temperature are expanded in Taylor series about the undisturbed state.

The equation governing the evolution of pure right-moving pulses may now be derived through a straightforward application of the method of multiple scales; the version used is essentially that described in Chapter IV of Leibovich & Seebass (1974). In terms of the variables (3.21) and (3.23), the resultant equation governing ρ_1 is found to be

$$\hat{\rho}_{\hat{t}} + (1 + \tfrac{1}{2}\hat{\rho})\hat{\rho}\hat{\rho}_{\hat{x}} = \frac{\delta \Lambda^2}{2\hat{\Gamma}^4}\hat{\rho}_{\hat{x}\hat{x}}, \tag{5.1}$$

where

$$\delta \equiv \frac{1}{\epsilon^2 R}\left(\frac{\lambda_0}{\mu_0} + 2 + \frac{\beta_0^2 T_0 a_0^2}{Pr\, c_{p0}}\right)$$

and $\beta_0 \equiv \bar{\beta}(\rho_0, s_0)$. The quantity δ is essentially the acoustic diffusivity for a general fluid; the conditions (2.8) and (2.10) ensure that $\delta > 0$ for all fluids considered here. A heuristic derivation of (5.1) would be to simply construct the left-hand side of (5.1) using the characteristic relations (3.14) and (3.15) or, alternatively, (4.1). The right-hand side can be taken directly from the linear theory for a general fluid. In his analysis of viscoelastic media, Lee-Bapty (1981) has derived the $\hat{\Gamma} = 0$ version

of (5.1), and a detailed discussion of the wave evolution of this equation is given by Crighton (1982).

Nimmo & Crighton (1982) have provided a comprehensive discussion of the application of Bäcklund transformations to a general class of parabolic equations. The conclusion of this study is that, except for relatively simple extensions of the classical (quadratic) Burgers equation, such transformations are not useful in generating exact solutions. Thus, in the absence of such exact procedures we have resorted to numerical techniques; these will be presented separately. Our main interest here is to use (5.1) to describe the continuum weak-shock structure for fluids in the vicinity of the transition zone. This may be formally derived by transforming to a coordinate system moving with the unknown shock speed S and then assuming that the shock structure is approximately steady in this coordinate system. When this is done, (5.1) becomes

$$\frac{\delta \Lambda^2}{2\hat{\Gamma}^4}\hat{\rho}_{\xi\xi} = \hat{\rho}\hat{\rho}_{\xi} + \tfrac{1}{2}\hat{\rho}^2\hat{\rho}_{\xi} - S\hat{\rho}_{\xi}, \tag{5.2}$$

where $\xi \equiv \hat{x} - S\hat{t}$. We now seek solutions $\hat{\rho} = \hat{\rho}(\xi)$ to (5.2) that satisfy

$$\left.\begin{aligned} \hat{\rho} &\to \hat{\rho}_{\mathrm{b}} \quad \text{as} \quad \xi \to \infty, \\ \hat{\rho} &\to \hat{\rho}_{\mathrm{a}} \quad \text{as} \quad \xi \to -\infty, \end{aligned}\right\} \tag{5.3}$$

and, for the sake of convenience, we will take

$$\hat{\rho}(0) = \tfrac{1}{2}(\hat{\rho}_{\mathrm{a}} + \hat{\rho}_{\mathrm{b}}).$$

Integration of (5.2) with respect to ξ yields a first-order equation governing $\hat{\rho}$. Furthermore, (5.3) can be used to verify the expected result that S is given by (4.2). If $\hat{\rho}$ and ξ are replaced by

$$G \equiv \frac{2}{[\hat{\rho}]}\left(\hat{\rho} - \frac{\hat{\rho}_{\mathrm{a}} + \hat{\rho}_{\mathrm{b}}}{2}\right), \quad \hat{\xi} \equiv \frac{\hat{\Gamma}^4 [\hat{\rho}]^2 \xi}{12\delta\Lambda^2}$$

it can be shown that G satisfies

$$G' = (G^2 - 1)(G + B), \tag{5.4}$$

where the prime denotes differentiation with respect to $\hat{\xi}$,

$$\left.\begin{aligned} &G \to -1 \quad \text{as} \quad \hat{\xi} \to \infty, \\ &G \to 1 \quad \text{as} \quad \hat{\xi} \to -\infty, \\ &G(0) = 0, \end{aligned}\right\} \tag{5.5}$$

and

$$B \equiv \frac{6}{[\hat{\rho}]}\left(1 + \frac{\hat{\rho}_{\mathrm{a}} + \hat{\rho}_{\mathrm{b}}}{2}\right). \tag{5.6}$$

A straightforward qualitative analysis shows that solutions for G satisfying (5.4) and (5.5) are possible only if $B \geqslant 1$. The significance of this result is seen by relating it to the shock and wave speeds. If we combine (5.6) with (4.1) and (4.2) it is easily shown that

$$\left.\frac{\mathrm{d}\hat{x}}{\mathrm{d}\hat{t}}\right|_{\mathrm{a}} - \frac{\mathrm{d}\hat{x}_{\mathrm{s}}}{\mathrm{d}\hat{t}} = \tfrac{1}{12}[\hat{\rho}]^2 (B + 1),$$

$$\frac{\mathrm{d}\hat{x}_{\mathrm{s}}}{\mathrm{d}\hat{t}} - \left.\frac{\mathrm{d}\hat{x}}{\mathrm{d}\hat{t}}\right|_{\mathrm{b}} = \tfrac{1}{12}[\hat{\rho}]^2 (B - 1).$$

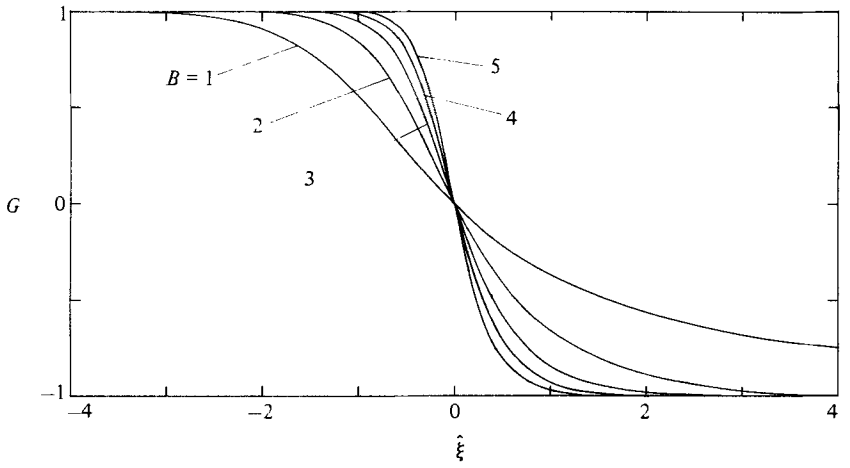

FIGURE 14. Shock structure. $B = 1.0$ corresponds to a shock having sonic conditions as $\hat{\xi} \to \infty$.

The condition that $B \geqslant 1$, i.e. that a viscous structure of the above form exists, therefore requires that (4.3) be satisfied for all admissible shocks. Thus the viscous evolution equation (5.1) not only yields the characteristic and shock speed relations found in §3 but also requires that the speed-ordering relation (3.19) and (3.20) or, equivalently, (4.3) be satisfied for all admissible shocks; in this sense the viscous theory is more complete than the weak shock theory.

Although the key result concerning the wave speeds and the fact that G is a monotonic transition between its asymptotes can be given through a qualitative analysis, we may also integrate (5.4) to obtain the details of the shock structure. For $B > 1$ we find that

$$\hat{\xi} = \frac{1}{B^2-1}\left\{2\ln\left(\frac{G}{B}+1\right)+B\ln\left(\frac{1-G}{1+G}\right)-\ln(1-G^2)\right\} \tag{5.7}$$

and for $B = 1$

$$\hat{\xi} = \tfrac{1}{2}\ln\frac{1-G}{1+G}-\frac{G}{1+G}. \tag{5.8}$$

It is easily seen that the case $B = 1$ corresponds to sonic conditions before the shock. Thus, when sonic conditions hold, the solution for G approaches the upstream asymptote algebraically in $\hat{\xi}$ rather than exponentially. This relatively slow approach is clear in figure 14, where (5.7) and (5.8) have been plotted. The original equation (5.4) can also be used to compute the position of the inflection point of (5.7) and (5.8). This is found to be

$$G = -\tfrac{1}{3}B+(\tfrac{1}{9}B^2+\tfrac{1}{3})^{\frac{1}{2}}.$$

Thus the additional nonlinearity in (5.4) shifts the inflection point downstream of the point where $\hat{\rho}$ attains its average value. This fact can also be seen by inspection of figure 14.

6. Summary

The propagation of small disturbances in a fluid having both positive ($\bar{\Gamma} > 0$) and negative ($\bar{\Gamma} < 0$) nonlinearity has been examined. The undisturbed state is taken to be in the vicinity of the transition line $\bar{\Gamma}(\bar{\rho}, \bar{s}) \equiv 0$. As a result, different parts of the wave could correspond to either positive or negative values of $\bar{\Gamma}$. The resultant wave evolution is seen to differ considerably from that of the classical theory; this is

primarily due to the fact that higher-order nonlinear terms must be included in even the lowest-order description. The evolution of inviscid and purely right-moving waves is governed by (3.14)–(3.16). Inadmissible shocks were eliminated through use of the inequalities (3.19) and (3.20). When dissipative effects are included, the evolution is governed by (5.1); this is recognized as an extension of the well-known Burgers equation. The shock-structure analysis shows that (5.1) not only contains the characteristic and shock-speed relations (3.14)–(3.16) but the admissibility conditions (3.19) and (3.20) as well.

Although the constitutive relations are simply those of a single-phase Navier–Stokes fluid, we find that shocks having either upstream or downstream sonic conditions are possible. The shock-structure analysis of §5 shows that the sonic conditions are approached algebraically rather than exponentially. We have also found that shocks exist in which the local value of the fundamental derivative $\bar{\Gamma}$ changes sign across the shock. This is seen to be in agreement with the remarks of Thompson & Lambrakis (1973).

The examples of §4 clearly suggest that, in spite of the complicated initial evolution, the ultimate decay of the waveform will always be that of the classical theory. The main exception to this is the case where $\hat{\Gamma} = 0$ and $\Lambda \neq 0$; here the shock amplitude decreases as the negative $\frac{1}{3}$-power of the propagation time.

The scope of the present study is confined to small-amplitude waves. However, we expect that many of the qualitative features and new phenomena discussed here will also be observed in large-amplitude waves for which the local value of $\bar{\Gamma}$ changes sign. Unfortunately, the double Chapman–Jouguet shock, i.e. where sonic conditions exist both upstream and downstream of the shock, is not contained in the present theory. The larger degree of nonlinearity necessary is typically contained only in shocks of moderate strength. We have also found that, when both $\hat{\Gamma}$ and Λ are simultaneously zero, a perturbation theory similar to the present theory may be developed which contains such shocks. The results obtained will be valid in a neighbourhood of the point where an isentrope is tangent to the transition line. Because of the even higher degree of nonlinearity, this theory is expected to contain most of the qualitative features of a moderate-strength theory although the timescales are of order of the negative-third power of the wave amplitude.

Finally, it is expected that much of the phenomena discussed here will also be found in fluids such as liquid helium in regions where the appropriate nonlinearity parameter is sufficiently small.

The authors would like to express their gratitude to H. B. Nguyen for his assistance in computation and plotting, one of the referees for pointing out the references concerning liquid helium, and D. G. Crighton for a number of valuable comments and references. One of the authors (A. Kluwick) gratefully acknowledges the hospitality of the Department of Engineering Science and Mechanics, Virginia Polytechnic Institute and State University, during the preparation of this work.

Appendix

As earlier, ρ, j, x and t denote the density, the related mass flux, the spatial coordinate and the time. In the most general case of a kinematic wave propagating into a homogeneous medium, the field quantities satisfy the continuity equation of the form

$$\frac{\mathrm{d}}{\mathrm{d}t}\int_{x_1(t)}^{x_2(t)} \rho(x',t)\,\mathrm{d}x + \dot{x}_1\rho(x_1,t) - \dot{x}_2\rho(x_2,t) = j(x_1,t) - j(x_2,t), \tag{A 1}$$

where $x_1(t)$ and $x_2(t)$ are arbitrary functions of t, and dots denote derivatives with respect to time. Equation (A 1) is recognized as a generalization of the conservation law used by Lighthill & Whitham (1955) and Kluwick (1977) to include the effects of a moving control volume. Furthermore, j and ρ are taken to satisfy the functional relationship

$$j = j(\rho). \tag{A 2}$$

Thus the flow is governed by the (kinematic) wave equation

$$\frac{\partial \rho}{\partial t} + v_w \frac{\partial \rho}{\partial x} = 0, \quad v_w = \frac{\mathrm{d}j}{\mathrm{d}\rho} \tag{A 3}$$

in regions where ρ and j are continuous and differentiable, while lines across which ρ and j change discontinuously propagate with the shock speed

$$v_s = \frac{[j]}{[\rho]}. \tag{A 4}$$

To specify solutions to (A 1) and (A 2) an initial condition

$$\rho(x, 0) = F(x) \tag{A 5}$$

will be imposed.

As is well known, the solution to the wave equation (A 3) subject to the initial condition (A 5) can be written in the form

$$\left.\begin{aligned} \rho &= F(\eta), \\ x &= \eta + v_w(\rho)\, t, \end{aligned}\right\} \tag{A 6}$$

where η is constant along characteristic lines $\mathrm{d}x/\mathrm{d}t = v_w$ provided that all characteristics η = constant emanate from the x-axis. If $\mathrm{d}v_w/\mathrm{d}\eta < 0$ inside some interval of the x-axis at $t = 0$, the distribution of the field variables (A 6) will become multivalued for

$$t > t_s = -\frac{1}{\dfrac{\mathrm{d}v_w(x, 0)}{\mathrm{d}x}} \tag{A 7}$$

where the maximum of the absolute value of the denominator has to be taken. For $t > t_s$, weak solutions to (A 1) and (A 2) have to be calculated in which these regions of multivaluedness are eliminated by the insertion of shock fronts. To this end it is convenient to determine first the stream function ψ satisfying

$$\rho = \frac{\partial \psi}{\partial x}, \quad j = -\frac{\partial \psi}{\partial t}. \tag{A 8}$$

Combination of (A 6) and (A 8) then yields

$$\psi = -\int_0^{\eta} F(x)\, \mathrm{d}x + (j - \rho v_w)\, t. \tag{A 9}$$

Since $x(\eta, t)$ and $\psi(\eta, t)$ are continuous across shock fronts (the latter condition being an immediate consequence of (A 4)), we obtain the conditions

$$\left.\begin{aligned} [\eta] + t[v_w] &= 0, \\ t[j - \rho v_w] &= -\int_{\eta_a}^{\eta_b} F(x)\, \mathrm{d}x, \end{aligned}\right\} \tag{A 10}$$

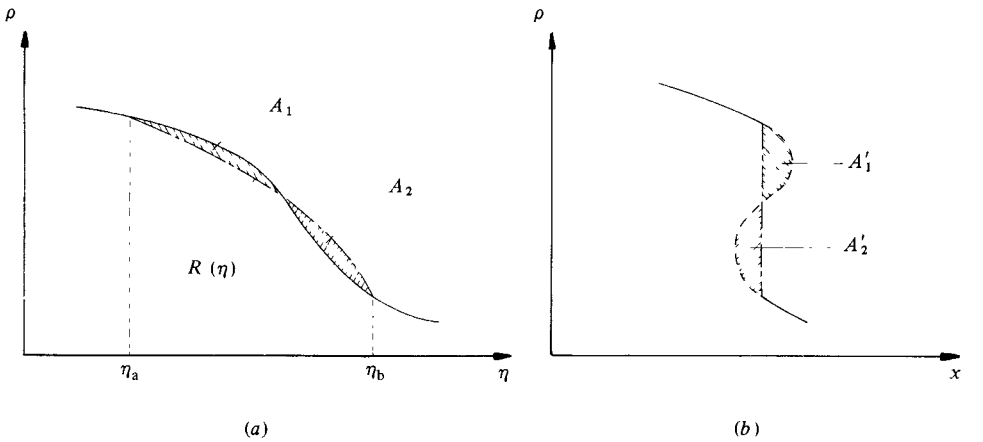

FIGURE 15. Generalized area rule: ——, density distributions at (*a*) $t = 0$ and (*b*) $t = t_1 > t_s$; – – – –, density distribution inside the multivalued region; ———, density distribution $R(\eta)$ that maps exactly into the shock discontinuity at $t = t_1$.

where η_a and η_b denote the values of the characteristics that merge with the shock at time t.

Elimination of t from (A 10) results in the following relationship between η_a and η_b:

$$\int_{\eta_a}^{\eta_b} F(x)\,\mathrm{d}x = [\eta]\frac{[j-\rho v_w]}{[v_w]}. \tag{A 11}$$

By solving for $\eta_a = \eta_a(\eta_b)$ say, by combining (A 6) with one of (A 10), then yields the curve of the shock front in the (x,t)-plane in parametric form: $x = x(\eta_a), t = t(\eta_a)$.

In the case of simple acoustic waves in a perfect gas $j = \frac{1}{2}\Gamma\rho^2$, (A 11) reduces to the well-known Whitham area rule (e.g. Whitham 1974). It is interesting to note, however, that (A 11) can be interpreted as an area rule even without this assumption.

This can be seen most easily if the following problem is treated first. For a given value of $t = t_1$ and corresponding values of η_a, η_b, let us replace the initial density distribution $F(\eta)$ inside $\eta_a \leqslant \eta \leqslant \eta_b$ by a different distribution $R(\eta)$ for which $F(\eta_a) = R(\eta_a)$, $F(\eta_b) = R(\eta_b)$ such that the new distribution is mapped into the shock discontinuity at $t = t_1$ (see e.g. figure 15). The problem of finding $R(\eta)$ is closely related to the problem to determine the density distribution inside a centred fan. Obviously it is necessary that all characteristics $\eta_a \leqslant \eta \leqslant \eta_b$ focus in one single point, which means that $v_w(R)$ has to vary linearly with η. Therefore $R(\eta)$ is defined implicitly by the requirement

$$v_w(R) = v_{wa} + (\eta-\eta_a)\frac{[v_w]}{[\eta]}. \tag{A 12}$$

Next let us calculate the total mass inside the interval $\eta_a \leqslant \eta \leqslant \eta_b$ following from (A 12). Using the relationship $\rho\,\mathrm{d}v_w = \mathrm{d}(j-\rho v_w)$ and (A 11) we obtain

$$\int_{\eta_a}^{\eta_b} R(x)\,\mathrm{d}x = \frac{[v_w]}{[\eta]}\int_{v_{wa}}^{v_{wb}} \rho\,\mathrm{d}v_w = \int_{\eta_a}^{\eta_b} F(x)\,\mathrm{d}x.$$

In the notation of figure 15 this result assumes the form of an area rule

$$A_1 = A_2. \tag{A 13}$$

Therefore the values η_a and η_b of characteristics that merge with the shock front at a certain time are related in such a way that the total mass inside the interval $\eta_a \leqslant \eta \leqslant \eta_b$ is equal to the total mass of the density distribution that maps exactly into the shock discontinuity at the same time. If the wave speed v_w is proportional to the density ρ, as in the case of classical gasdynamics, (A 12) leads to a linear density distribution in agreement with Whitham's area rule. For the problem considered in this study, one obtains

$$R(\eta) = -1 \pm \left[(1+\hat{\rho}_a)^2 - 2\frac{\eta-\eta_a}{\hat{t}_1} \right]^{\frac{1}{2}}. \tag{A 14}$$

Comparison of (A 14) with (3.24) once more shows the close relationship of the density distribution entering the formulation of the area rule and that inside a centred wave fan.

It has been shown by Lighthill (1957) that the continuity of the stream function across shock fronts leads to the area rule of Landau when ρ is plotted as a function of x for fixed t. Using the notation of figure 15, this area rule can be expressed in the form

$$A_1' = A_2'. \tag{A 15}$$

The above considerations then indicate the close relationship between the area rules (A 11) and (A 15). Equation (A 11) follows directly from (A 15) by calculating the corresponding initial distribution using the integrated slope condition (A 6). At this point, however, a limitation of (A 11) and its equivalence with Landau's area rule has to be noted. Since the derivation of (A 11) is based on the integrated slope condition (A 6), the above considerations are valid only as long as the characteristics η_a and η_b both intersect the x-axis. In general this requirement is no longer satisfied if the shock speed is equal to one of the characteristic wave speeds immediately upstream and downstream of the shock front, and (A 11) ceases to be valid. Thus, when sonic conditions hold, only Landau's area rule can be applied, while the generalization of Whitham's rule (A 13) cannot.

REFERENCES

Barker, L. M. & Hollenbach, R. E. 1970 Shock-wave studies of PMMA, fused silica, and sapphire. *J. Appl. Phys.* **41**, 4208–4226.

Bethe, H. A. 1942 The theory of shock waves for an arbitrary equation of state. *Office Sci. Res. & Dev. Rep.* 545.

Bezzerides, B., Forslund, D. W. & Lindman, E. L. 1978 Existence of rarefaction shocks in a laser-plasma corona. *Phys. Fluids* **21**, 2179–2185.

Borisov, A. A., Borisov, Al. A., Kutateladze, S. S. & Nakorykov, V. E. 1983 Rarefaction shock wave near the critical liquid–vapour point. *J. Fluid Mech.* **126**, 59–73.

Courant, R. & Friedrichs, K. O. 1948 *Supersonic Flow and Shock Waves*. Springer.

Crighton, D. G. 1982 Propagation of non-uniform shock waves over large distances. In *Proc. IUTAM Symp. on Nonlinear Deformation Waves* (ed. U. Nigul & J. Engelbrecht). Springer.

Dessler, A. J. & Fairbank, W. M. 1956 Amplitude dependence of the velocity of second sound. *Phys. Rev.* **104**, 6–10.

Garrett, S. 1981 Nonlinear distortion of 4th sound in superfluid ^{3}He-B. *J. Acoust. Soc. Am.* **60**, 139–144.

Germain, P. 1972 Shock waves, jump relations and structure. *Adv. Appl. Mech.* **12**, 131–134.

Hayes, W. D. 1960 Gasdynamic discontinuities. *Princeton Series on High Speed Aerodynamics and Jet Propulsion*. Princeton University Press.

HIRSCHFELDER, J. O., BUEHLER, R. J., MCGEE, H. A. & SUTTON, J. R. 1958 Generalized thermodynamic excess functions for gases and liquids. *Ind. Engng Chem.* **50**, 386.

KHALATNIKOV, I. M. 1952 Discontinuities and large amplitude sound waves in helium II. *Zh. Eksp. Teor. Fiz.* **23**, 253.

KHALATNIKOV, I. M. 1965 *Introduction to the Theory of Superfluidity*. Benjamin.

KLUWICK, A. 1977 Kinematische Wellen. *Acta Mech.* **26**, 15–46.

LAX, P. D. 1971 Shock waves and entropy. In *Contributions to Nonlinear Functional Analysis* (ed. E. H. Zarantonello). Academic.

LEE-BAPTY, I. P. 1981 Ph.D. dissertation, Leeds University, England.

LEIBOVICH, S. & SEEBASS, A. R. 1974 *Nonlinear Waves*. Cornell University Press.

LIGHTHILL, M. J. 1957 River waves. *Nav. Hydrodyn. Publ.* **515.** Natl Acad. Sci., Natl Res. Council.

LIGHTHILL, M. J. & WHITHAM, G. B. 1955 On kinematic waves. I. Flood movement in long rivers. *Proc. R. Soc. Lond.* A **229**, 281–316.

MARTIN, J. J. & HOU, Y. C. 1955 Development of an equation of state for gases. *AIChE J.* **1**, 142.

NIMMO, J. J. C. & CRIGHTON, D. G. 1982 Bäcklund transformations for nonlinear parabolic equations: the general results. *Proc. R. Soc. Lond.* A **384**, 381–401.

OSBORNE, D. V. 1951 Second sound in liquid helium II. *Proc. Phys. Soc. Lond.* A **64**, 114–123.

TAYLOR, G. I. 1910 The conditions necessary for discontinuous motion in gases. *Proc. R. Soc. Lond.* A **84**, 371–377.

TEMPERLEY, H. N. V. 1951 The theory of propagation in liquid helium II of 'temperature waves' of finite amplitude. *Proc. Phys. Soc. Lond.* A **64**, 105–114.

THOMPSON, P. A. 1971 A fundamental derivative in gasdynamics. *Phys. Fluids* **14**, 1843–1849.

THOMPSON, P. A. & LAMBRAKIS, K. C. 1973 Negative shock waves. *J. Fluid Mech.* **60**, 187–208.

WHITHAM, G. B. 1974 *Linear and Nonlinear Waves*. Wiley-Interscience.

ZEL'DOVICH, YA. B. 1946 On the possibility of rarefaction shock waves. *Zh. Eksp. Teor. Fiz.* **4**, 363–364.